

JAERI-M
93-159

THERMAL CYCLIC OXIDATION BEHAVIOR OF THE
DEVELOPED COMPOSITIONALLY GRADIENT
GRAPHITE MATERIAL OF SiC/C IN AIR
ENVIRONMENT

August 1993

Junichi NAKANO, Kimio FUJII
and Masami SHINDO

JAERI Mレポートは、日本原子力研究所が不定期に公開している研究報告書です。
入手の間合わせは、日本原子力研究所技術情報部情報資料課 〒319-11 茨城県那珂郡東海村にお申しこみください。なお、このほか財団法人原子力弘済会資料センター 〒319-11 茨城県那珂郡東海村日本原子力研究所内で複写による実費頒布をおこなっております。

JAERI M reports are issued irregularly.
Inquiries about availability of the reports should be addressed to Information Division Department of Technical Information, Japan Atomic Energy Research Institute, Tokaimura, Naka gun, Baraki ken 319-11, Japan.

© Japan Atomic Energy Research Institute, 1993

編集兼発行 日本原子力研究所
印刷 ニッセイエプロ株式会社

Thermal Cyclic Oxidation Behavior of the
Developed Compositionally Gradient Graphite
Material of SiC/C in Air Environment

Junichi NAKANO, Kimio FUJII and Masami SHINDO

Department of Materials Science and Engineering
Tokai Research Establishment
Japan Atomic Energy Research Institute
Tokai-mura, Naka-gun, Ibaraki-ken

(Received July 20, 1993)

For the developed compositionally gradient graphite material composed of surface SiC coating layer, middle SiC/C layer and graphite matrix, the thermal cyclic oxidation test was performed together with two kinds of the SiC coated graphite materials in air environment.

It was made clear that the developed material exhibited high performance under severe thermal cyclic condition independent of the morphology of middle SiC/C layers and had the longer time or the more cycle margins from crack initiation to failure for surface SiC coating layer compared with the SiC coated graphite materials.

Keywords : Compositionally Gradient Material, SiC, SiC Coating,
Thermal Cyclic Oxidation, Oxidation Resistance,
Thermal Cyclic Resistance, Advanced Carbon and
Graphite Materials

SiC/C 傾斜組成黒鉛開発材料の空気中における熱サイクル酸化挙動

日本原子力研究所東海研究所材料研究部

中野 純一・藤井貴美夫・新藤 雅美

(1993年7月20日受理)

表面 SiC 被覆層、SiC/C 中間層及び黒鉛基地から構成される傾斜組成黒鉛開発材料について、2種類の SiC 被覆黒鉛材料とともに空気中で苛酷な熱サイクル酸化試験を実施した。

開発材料は、中間層である SiC/C の形態によらず厳しい熱サイクル酸化条件下でも優れた特性を示すこと及び SiC 被覆黒鉛材料に比較して表面 SiC 被覆層の亀裂発生から破損に至る時間的余裕が長い或いはサイクル数的余裕が多いことを明らかにした。

Contents

1. Introduction	1
2. Experimental Procedure	2
2.1 Materials	2
2.2 Thermal Cyclic Oxidation Test	3
3. Results and Discussion	4
3.1 Comparison among Materials	4
3.2 Mass Loss Behavior	6
3.3 Influence of Middle SiC/C Layer's Morphology	7
4. Summary and Conclusions	8
References	9

目 次

1. 緒 言	1
2. 実験手順	2
2.1 材 料	2
2.2 熱サイクル酸化試験	3
3. 結果及び討論	4
3.1 材料間の比較	4
3.2 重量減少挙動	6
3.3 SiC/C 中間層の形態の影響	7
4. まとめ及び結論	8
参考文献	9

1. INTRODUCTION

The development study of advanced carbon and graphite materials, which are a kind of high oxidation resistant material including thermal cyclic resistance, has been carried out [1,2]. The compositionally gradient material of SiC/C as advanced carbon and graphite materials is being developed both for improvement of the oxidation resistance and for relaxation of the thermal stress induced in the material under thermal cycle, thermal shock, etc. in aggressive environments.

The developed compositionally gradient graphite material of SiC/C composed of surface SiC coating layer, middle SiC/C layer and graphite matrix, in which the SiC concentration gradually decreases from the surface to the inside, exhibited an excellent oxidation characteristic with thermal cyclic resistance at high temperatures in air [2]. And although the number of tested samples was only a few, the fruitful prospect for development of high oxidation resistant carbon and graphite materials could be obtained from the previous report [2].

The compositionally gradient material of SiC/C is produced by the following two processes ; ① The first process is to form the middle SiC/C layer at the near surface of substrate carbon and graphite materials by the reaction between carbon and gaseous SiO. The formed SiC/C layer has a gradient in concentration of SiC due to surface and in-pore diffusion reactions. ② The second process is to coat SiC by chemical vapor deposition method on the middle SiC/C layer. Finally, the compositionally gradient material of SiC/C, which is composed of surface SiC coating layer, middle SiC/C layer and graphite matrix, is completed.

The integrity, the reliability, etc. of the produced compositionally gradient material are strongly dependent on the adhesion, the stability, etc. of surface SiC coating layer. And for these characteristics of surface SiC coat-

ing layer the morphology of the substrate, i.e., middle SiC/C layer, may be one of the key factors.

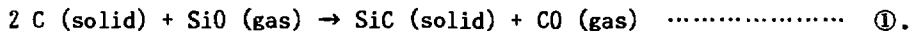
This study aims to confirm the high performance of the developed compositionally gradient graphite material including the influence of morphology of middle SiC/C layers compared with two kinds of SiC coated graphite materials under severe thermal cyclic oxidative condition.

2. EXPERIMENTAL PROCEDURE

2.1. Materials

2.1.1. Compositionally gradient graphite material of SiC/C

Materials used for the formation of middle SiC/C layer were an isotropic fine-grained nuclear grade graphite, IG-110 graphite (Toyo Tanso Co., Ltd.), and solid SiO of 99.9 % purity. The graphite sample was in the form of a cylinder, 20 mm in length and 10 mm in diameter, with convex sides (2 R & 4 R). Solid SiO in powder form changes into gaseous SiO at high temperature in inert environments. The middle SiC/C layer was formed by the following reaction in a high purity helium stream at the reaction temperature of 1380 °C and the SiO gasification temperature of 1300 °C,



After the reaction ①, the mass gain was observed due to the formation of SiC. Larger mass gain means higher SiC concentration and deeper SiC/C layer in the graphite sample. However, the excessive mass gain, e.g., around 3 %, induced the failure of sample caused by volume expansion [1].

For the study of influence of the morphology of middle SiC/C layer on the adhesion and the stability of surface SiC coating layer, the graphite materials with various SiC/C layers (SiC/C), mass gains of which were 0.37-2.66 %,

were prepared by controlling the reaction time of the formula ①.

The compositionally gradient graphite materials of SiC/C, i.e., SiC coated the SiC/C (SiC-SiC/C), is produced by chemical vapour deposited (CVD) SiC coating on the SiC/C. The SiC coating thickness by CVD was around 100 μm .

2.1.2. SiC coated graphite materials

Two kinds of SiC coated graphite materials were produced by CVD SiC coating with same coating condition as that on the SiC/C. One of two substrate graphite is the same one as the basic material, IG-110 graphite, of the SiC-SiC/C. The other is SiC-6 graphite (brand name of Toyo Tanso Co., Ltd.) which is the fittest graphite for surface SiC coating because that the thermal expansion coefficient is about the same as that of β -SiC. Both the graphite samples were also in the form of a cylinder, 20 mm in length and 10 mm in diameter, with convex sides (4 R). In this connection, the values of thermal expansion coefficient for β -SiC, IG-110 graphite and SiC-6 graphite are $4.7 \times 10^{-6}/\text{K}$ (293-2400 K) [3], $4.1 \times 10^{-6}/\text{K}$ (293-673 K) [4] and $5.0 \times 10^{-6}/\text{K}$ (623-723 K) [5], respectively.

Moreover, it was identified by X-ray analysis, etc. that both the SiC coated by CVD and formed by the reaction ① had a structure of β -SiC crystal.

The all surface SiC coatings by CVD were performed by the outside with taking account of the temperature of basic materials is kept lower than 1380 $^{\circ}\text{C}$ of the reaction ① because of the maintenance of SiC/C compositionally gradient in the SiC/C.

2.2. Thermal Cyclic Oxidation Test

For all specimens the thermal cyclic oxidation test was carried out. In

the test, the specimens were heated with a heating rate of 20 °C/s up to 1020 °C and kept at this temperature for 5 min in air, and then water-quenched in distilled water of 20 °C. The thermal cycle was repeated till the surface SiC coating layer was completely failed, in other words till the mass of specimen decreased over 10 % of the original mass. Isothermal heating, which was conducted at 800 °C in air for 1 h, was continued for evaluation of the integrity of surface SiC coating layers after each thermal cycle.

Prior to the thermal cyclic oxidation test, for all specimens the preheat treatment at 800 °C for 1 h in air is given in order to confirm the integrity of as-received SiC coating layers. And only the sound specimens shown no mass change were tested.

In the case of that the SiC coating layer is damaged and/or failed by the thermal cycle, the specimen shows mass loss mainly by reason of the oxidation of substrate graphite through the cracks in the SiC coating layer and/or at the parts of spalled SiC coating layer during the isothermal heating.

The thermal cyclic oxidation behavior for all tested samples was principally evaluated by mass change measurement before and after each thermal cycle and the isothermal heating. The evaluation process by mass measurement is illustrated in fig.1.

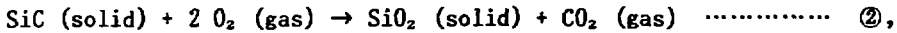
3. RESULTS AND DISCUSSION

3.1. Comparison among Materials

The mass loss curves of the SiC-SiC/C plotted as a function of cumulated isothermal heating time and number of cycles are given in fig. 2 compared with those of the SiC coated IG-110 (SiC-IG-110). Fig. 3 shows the mass loss curves of the SiC coated SiC-6 (SiC-SiC-6) together with the data range for the SiC-SiC/C. Figs. 2 and 3 indicated that the characteristic of the SiC-SiC/C against

thermal cycle was more stable than that of the SiC-IG-110 and a little inferior to that of the SiC-SiC-6.

SiC is oxidized by the following reaction in air,



and the formed very thin SiO₂ layer on SiC is very stable up to around 1000°C [6]. During the surface SiC coating layer maintains its integrity, the specimen exhibits no significant mass loss [2]. The observed mass loss is, therefore, related to the damage and/or the failure of surface SiC coating layer.

The damage and/or the failure of coating layer mainly results from the thermal stress induced at an interface due to the difference of the thermal expansion coefficients between the coating layer and the substrate material.

For the SiC-SiC/C the induced thermal stress hardly concentrates at a certain place because of the existence of SiC/C layer as a wide interface between the surface SiC coating layer and the substrate graphite (see fig. 4 (a)). Moreover, the initiated place of crack might be not the macroscopic interface between surface SiC coating layer and middle SiC/C layer but the microscopic interface between SiC and C in the middle SiC/C layer.

The different mass loss behavior between the SiC-IG-110 and the SiC-SiC-6, which have clear interfaces as a line (see fig. 4 (b)), is caused by the different thermal expansion coefficients of both substrate graphite materials. Since the value of thermal expansion coefficient, $5.0 \times 10^{-6}/\text{K}$, of SiC-6 graphite is nearly the same as that, $4.7 \times 10^{-6}/\text{K}$, of β -SiC compared with that, $4.1 \times 10^{-6}/\text{K}$, of IG-110 graphite, the induced thermal stress at the interface between SiC coating layer and SiC-6 was minimized. Otherwise the stresses induced in SiC coating layers on both graphite materials at a cooling process show different directions, i.e., the stresses for the SiC-SiC-6 and the SiC-IG-110 are compressive and tensile ones, respectively, because of the large and small relationship of the thermal expansion coefficients between β -SiC and SiC-6 or IG-110. The stress directions induced in SiC coating layers and substrate materials at

cooling process is conceptionally illustrated in fig. 5. The different stress directions in SiC coating layers on both graphite might also give the different mass loss behavior between the SiC-SiC-6 and the SiC-IG-110.

In conclusion, the SiC-SiC/C, which has no clear interface as a line, and the SiC-SiC-6, which is used the most fitted graphite for SiC coating as the substrate material, exhibit more stable characteristic against severe thermal cycle.

3.2. Mass Loss Behavior

From the curves in figs. 2 and 3, it can be seen that the SiC-SiC/C has a time or a cycle margins from significant mass loss to rapid mass loss compared with two kinds of SiC coated graphite materials. For more detailed information on the time or the cycle margins, the significant mass loss and the rapid mass loss were defined by a crack initiation in surface SiC coating layer and a failure (or spallation) of surface SiC coating layer, respectively. Expressing in figures, the crack initiation, i.e., a point shown significant mass loss, is the time or the number of cycles given about 0.2 % mass loss, and the failure (or spallation), i.e., a transition point shown rapid mass loss, is the time or the number of cycles given about 1.8 % mass loss.

The time or the number of cycles to crack initiation (a), the time or the number of cycles to failure (b) and the time or the cycle margin from crack initiation to failure (b-a) for the surface SiC coating layers of all tested specimens are summarized in table 1. For convenience, these times plotted as a function of mass gains of the SiC/C are shown in figs. 6, 7 and 8 together with comparative data for the SiC-SiC-6 and the SiC-IG-110, respectively. As can be seen these figures, the times to crack initiation and to failure of the SiC-SiC/C are so later than those of the SiC-IG-110 and a little earlier than those of the SiC-SiC-6, and the time margins from crack initiation to failure

of the SiC-SiC/C are much longer than those of both the SiC coated graphite materials.

The longer time margin of the SiC-SiC/C might be caused by the substrate conditions beneath the surface SiC coating layer. The mass loss is directly related to the oxidation of substrate materials through the cracks initiated in the surface SiC coating layer and at the parts of spalled SiC coating layer. Fig. 9 [1] shows the oxidation behavior of both the substrate materials, i.e., the SiC/C and IG-110 graphite, at 800°C in air, which indicated that the oxidation rate of the SiC/C was lower than those of graphite materials. Therefore, for both the SiC-IG-110 and the SiC-SiC-6 the substrate graphite beneath the surface SiC coating layer is rapidly oxidized by oxygen through the cracks as soon as cracks initiated in the SiC layers and then the SiC layer peels off immediately due to the loss of substrate. After the spallation of surface SiC coating layer, the mass decreases violently caused by the direct oxidation reaction between substrate graphite and oxygen.

The discussion mentioned above on the process from crack initiation to failure for surface SiC coating layers of the SiC-SiC/C and both the SiC coated graphite materials (SiC-C) is schematically illustrated in fig. 10.

The conclusion is that the slow oxidation rate of the SiC/C as substrate material by oxygen through the cracks in surface SiC coating layer leads the longer time margin from crack initiation to failure for the surface SiC coating layer on the SiC-SiC/C.

3.3. Influence of Middle SiC/C Layer's Morphology

With respect to the influence of morphology of middle SiC/C layer on the adhesion and the stability of the surface SiC coating layer, as can be seen from figs. 6, 7 and 8, the time to crack initiation, the time to failure and the time margin from crack initiation to failure were independent of the mass gain, i.e.,

the morphology of middle SiC/C layer. It seemed that these characteristics of surface SiC coating layer were related to the oxidation characteristic of the SiC/C, especially after crack initiation, however even the time margin did not depend on the mass gain. Larger mass gain directly contributes to increasing of the SiC concentration and of the porosity in the middle SiC/C layer. The oxidation rate of the SiC/C must decrease with increasing the SiC concentration and increase with increasing the porosity. It has already been confirmed that although the oxidation rate of the SiC/C is lower than those of virgin graphite materials as shown in fig. 9, the rate is independent of the mass gain.

It can be concluded that the adhesion and the stability of surface SiC coating layer on the SiC/C does not depend on the morphology of middle SiC/C layer due to the counterbalanced effect between the increase of SiC concentration as an advantage and the increase of porosity as a disadvantage.

4. SUMMARY AND CONCLUSIONS

For the confirmation of high performance of the developed SiC-SiC/C composed of surface SiC coating layer, middle SiC/C layer and graphite matrix including the influence of morphology of middle SiC/C layers, the thermal cyclic oxidation test for many kinds of the SiC-SiC/C, which have different SiC/C layers, and two kinds of SiC coated graphite, i.e., the SiC-IG-110 and the SiC-SiC-6, were performed in aggressive oxidative environment. The conclusions obtained showed that:

- (1) The SiC-SiC/C exhibited an excellent thermal cyclic resistance under severe thermal cyclic condition.
- (2) The SiC-SiC/C had the longer time or the more cycle margins from crack initiation to failure for the surface SiC coating layer compared with both the SiC coated graphite materials, although the times or the number of cycles to crack initiation and to failure were a little earlier than those of the

SiC-SiC-6 used the fittest graphite for SiC coating as the substrate.

(3)The adhesion and the stability of surface SiC coating layer for the SiC-SiC /C were independent of the morphology of middle SiC/C layer.

REFERENCES

- [1] K. Fujii, H. Imai, S. Nomura and M. Shindo, J. Nucl. Mater. 137(1992)204.
- [2] K. Fujii, J. Nakano and M. Shindo, Improvement of the oxidation resistance of a graphite material by compositionally gradient SiC/C layer, J. Nucl. Mater. in press.
- [3] G. V. Samsonov and I. M. Vinitiskij, Data Book for High Melting Point Compounds, translated into Japanese by the Translation Group of Nisso Tsushinsha, Nisso Tsushinsha (1976)p.217.
- [4] T. Iyoku, S. Shiozawa, M. Ishihara, T. Arai and T. Oku, Nucl. Eng. Des. 132(1991)23.
- [5] Graphite Applications, Catalog of Toyo Tanso Co., Ltd.
- [6] K. Motzfeldt, Acta Chem. Scand. 18(1964)1596.

Table 1 Time or number of cycles to crack initiation in SiC coating layer (a), time or number of cycles to failure of SiC coating layer (b) and time or cycle margins from crack initiation to failure for SiC coating layer (b-a) of all tested specimens.

Specimen and mass gain of SiC/C (%)	Crack initiation (0.2% mass loss) h & (cycles)	Failure (1.8% mass loss) h & (cycle)	Margin h & (cycle)
<u>SiC-SiC/C(2R)</u>			
0. 3 7	45.0 (42)	74.5 (69)	29.5 (27)
0. 3 9	37.0 (35)	64.0 (60)	27.0 (25)
1. 3 2	23.5 (22)	47.5 (44)	24.0 (22)
2. 0 8	36.5 (34)	53.0 (49)	16.5 (15)
<u>SiC-SiC/C(4R)</u>			
0. 9 8	38.0 (36)	63.0 (59)	25.0 (23)
1. 0 0	29.5 (28)	58.5 (54)	29.0 (26)
1. 2 1	33.0 (31)	65.0 (60)	32.0 (29)
1. 4 5	39.5 (37)	63.0 (59)	23.5 (22)
2. 6 6	60.5 (56)	111.5(103)	51.0 (47)
0. 3 8	26.5 (25)	56.0 (52)	29.5 (27)
<u>SiC-IG-110</u>			
① no SiC/C	7.0 (7)	10.0 (10)	3.0 (3)
② "	1.5 (2)	3.5 (4)	2.0 (2)
③ "	2.5 (3)	4.0 (4)	1.5 (1)
④ "	4.5 (5)	5.5 (6)	1.0 (1)
<u>SiC-SiC-6</u>			
① no SiC/C	83.5 (78)	84.5 (78)	1.0 (0)
② "	38.5 (36)	43.5 (41)	5.0 (5)
③ "	73.0 (68)	76.0 (71)	3.0 (3)
④ "	69.5 (65)	70.5 (66)	1.0 (1)

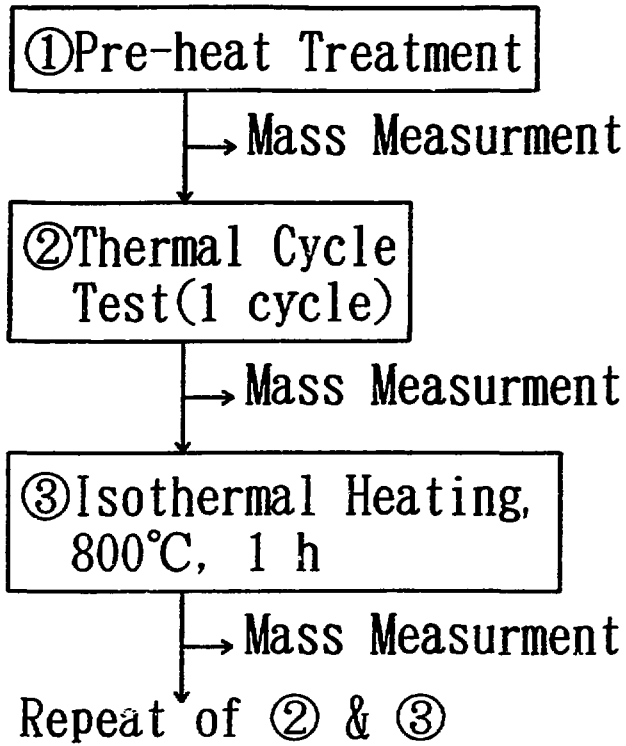


Fig. 1 Evaluation process by mass measurement for thermal cyclic oxidation test.

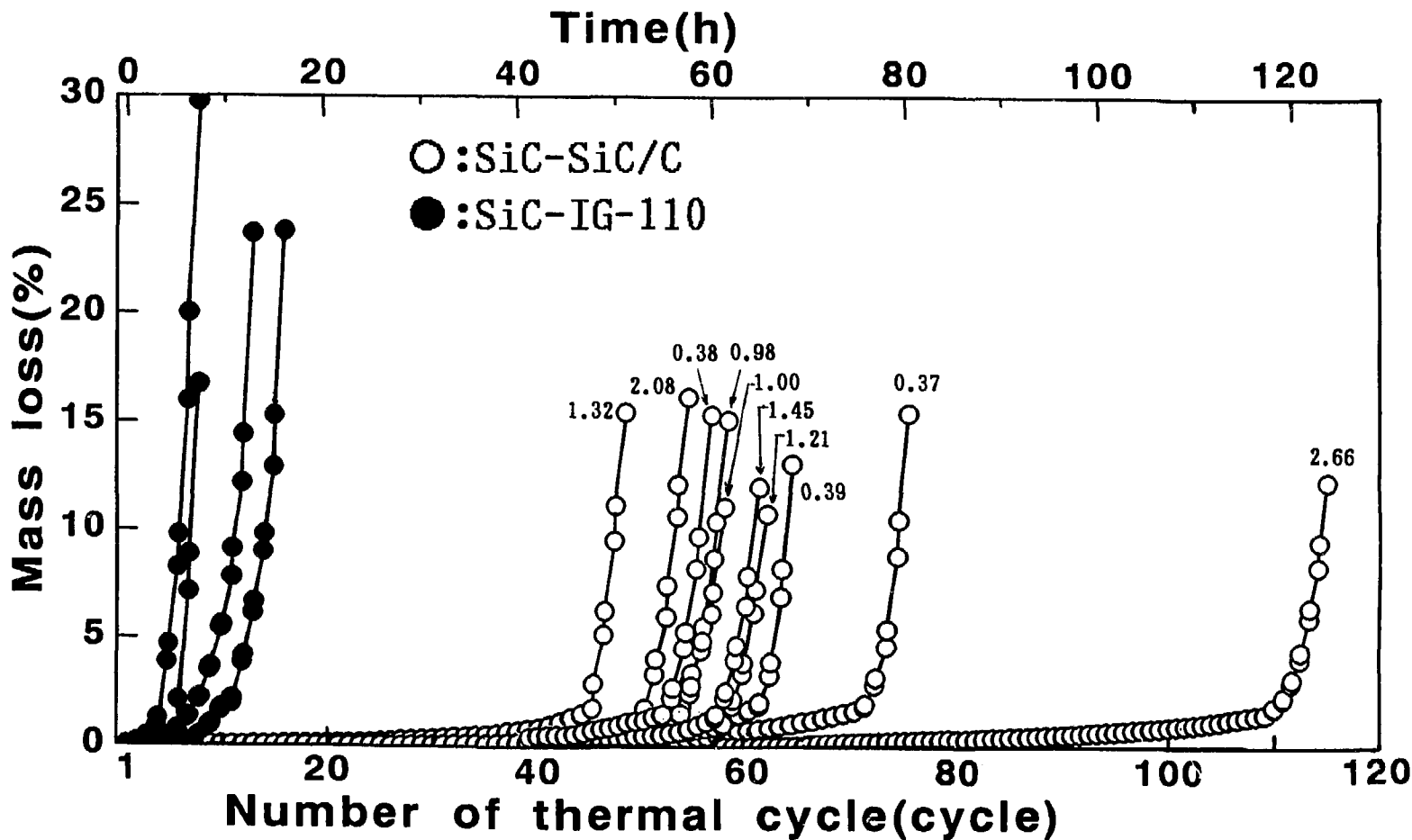


Fig. 2 Mass loss curves of the SiC-SiC/C together with comparative data for the SiC-IG-110. Figures by data of the SiC-SiC/C are mass gain (%) of the SiC/C.

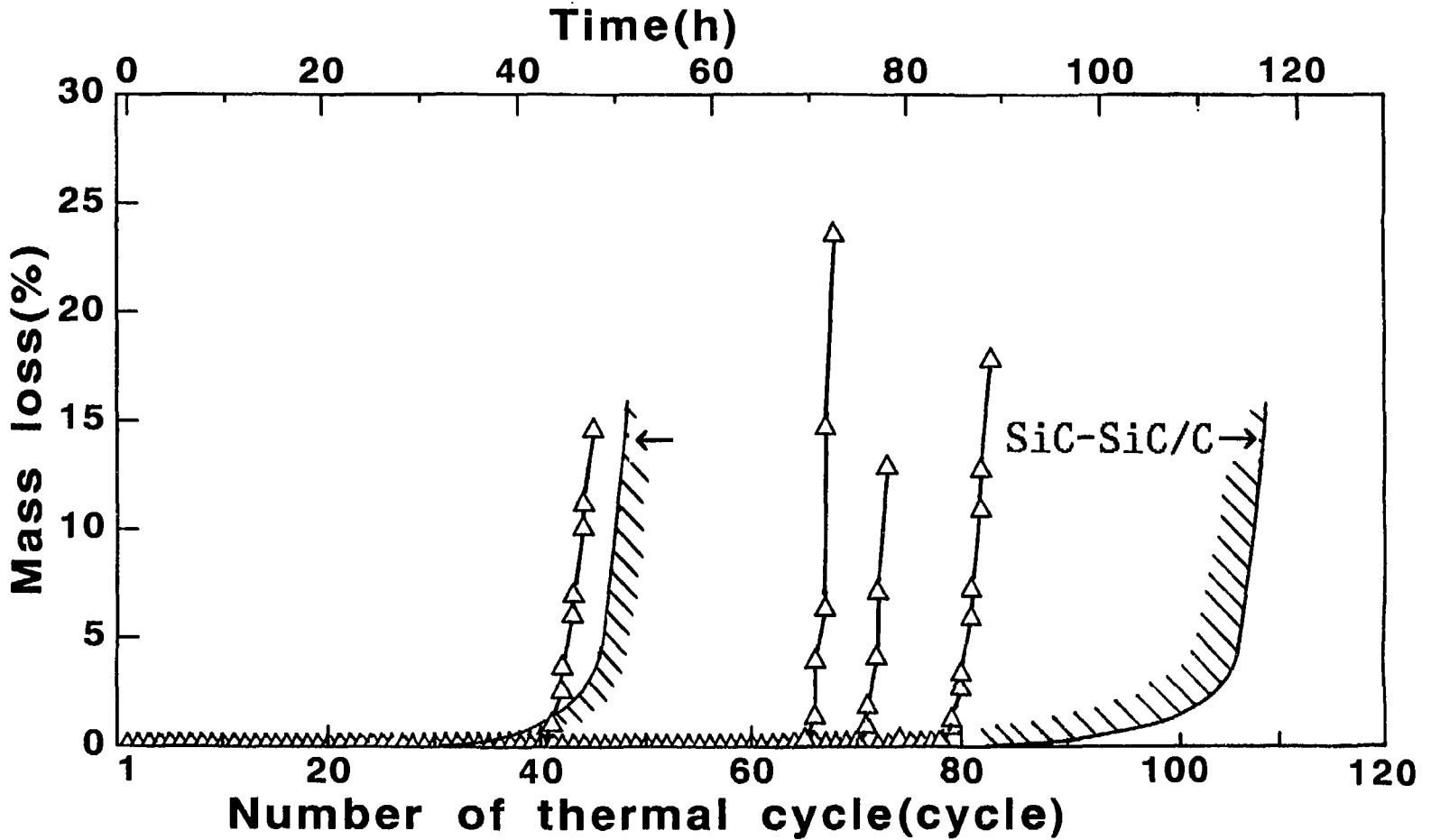


Fig. 3 Mass loss curves of the SiC-SiC-6 together with the data range for the SiC-SiC/C.

(a) SiC-SiC/C

(b) SiC-IG-110

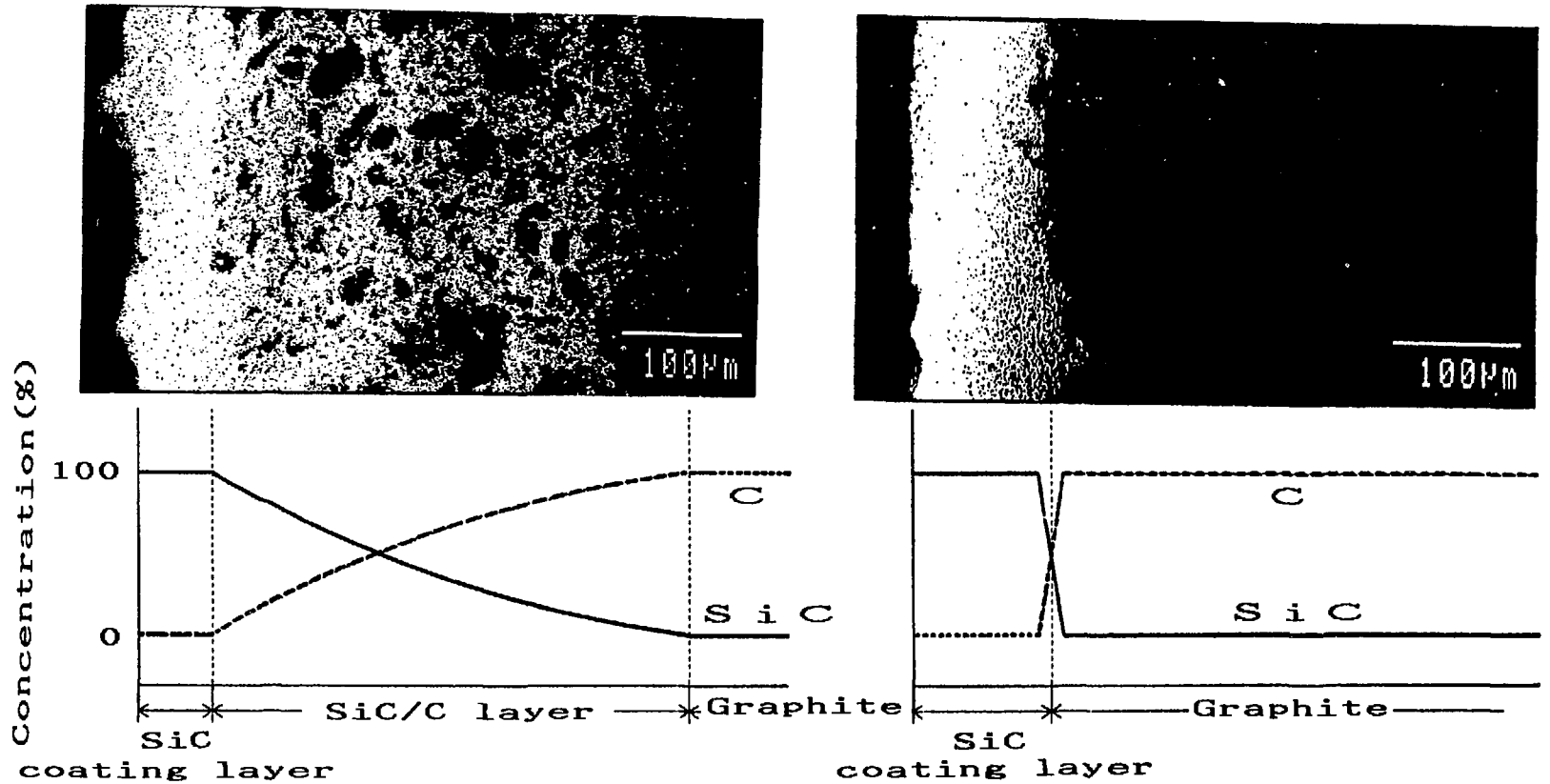
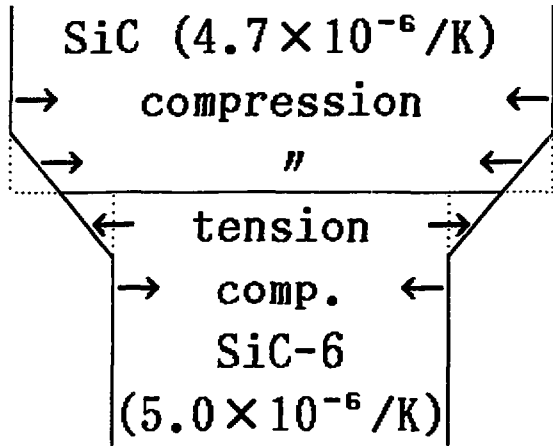


Fig. 4 Characteristic X-ray images of Si and conceptional model of changes in concentrations of SiC and C for cross sections of the SiC-SiC/C (a) and the SiC-IG-110 (b).

(a) SiC-SiC-6



(b) SiC-IG-110

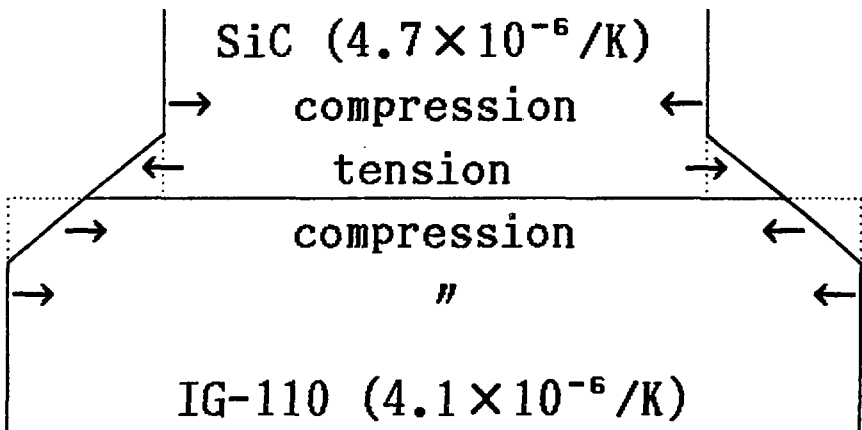


Fig. 5 Conceptual model of induced stress directions in SiC coating layers and substrate materials of SiC-SiC-6 and SiC-IG-110 at cooling process.

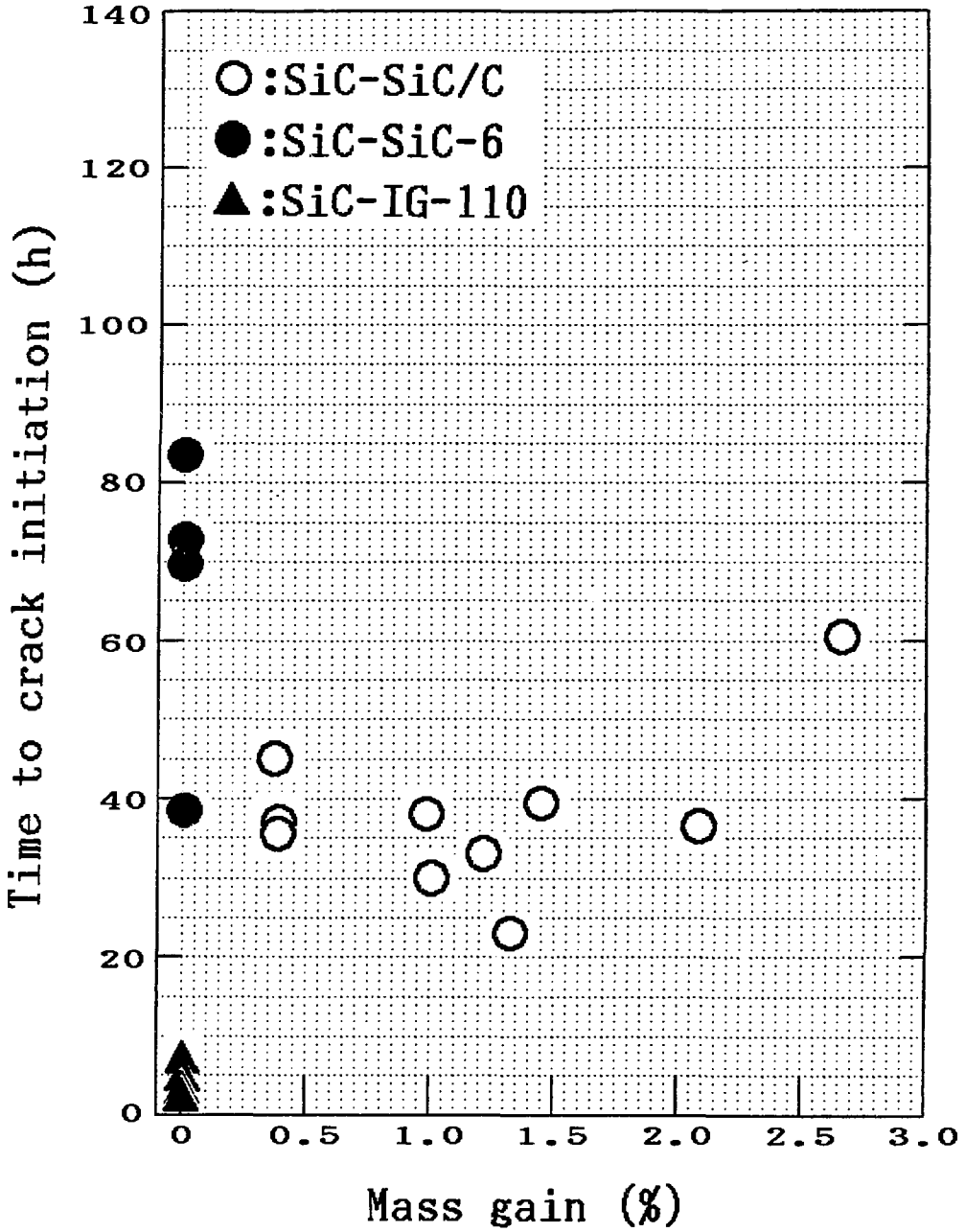


Fig. 6 Time to crack initiation in SiC coating layer of the SiC-SiC/C as a function of mass gain of the SiC/C together with comparative data for both SiC coated graphite materials (without the SiC/C layer).

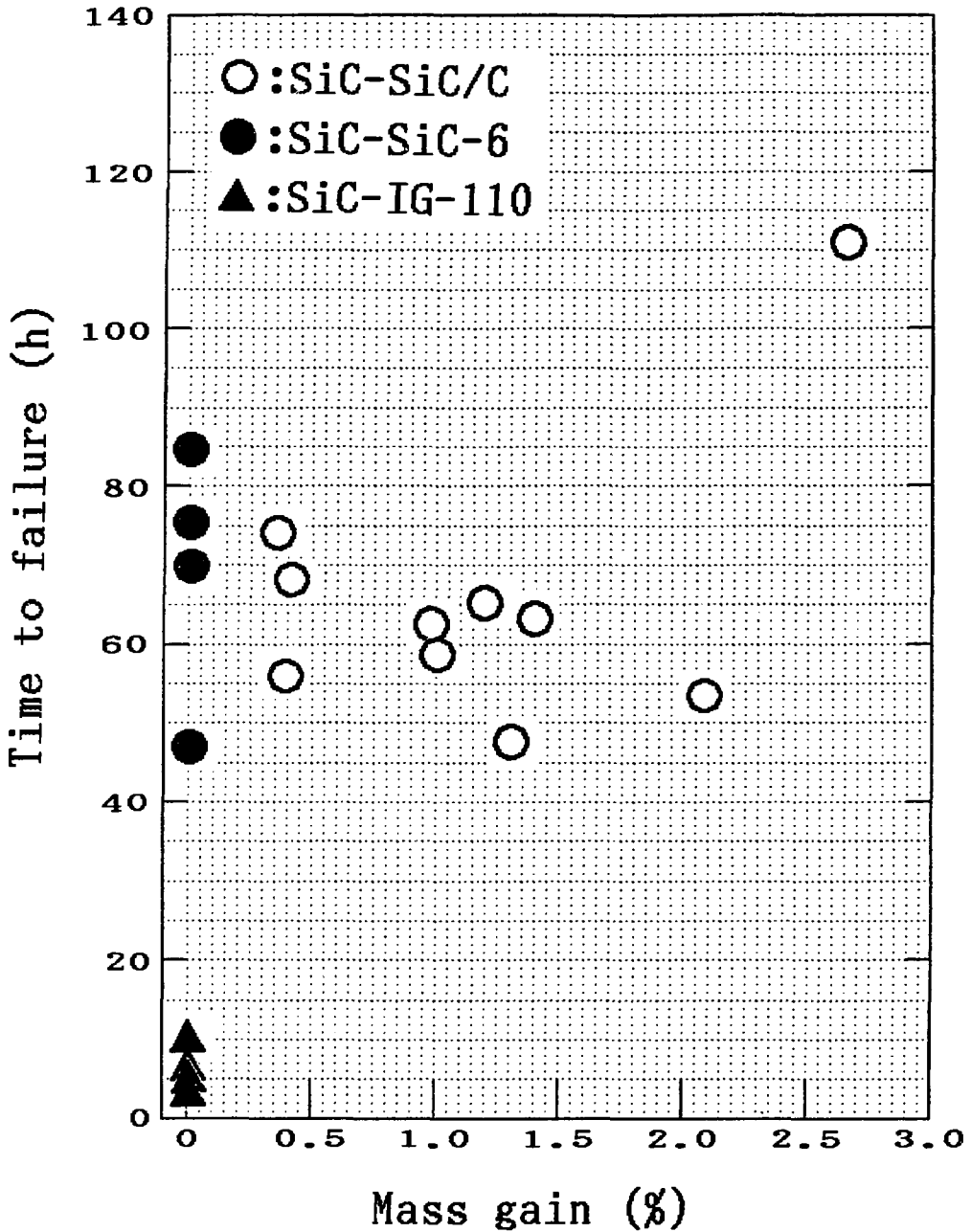


Fig. 7 Time to failure of surface SiC coating layer of the SiC-SiC/C as a function of mass gain of the SiC/C together with comparative data for both SiC coated graphite materials (without the SiC/C layer).

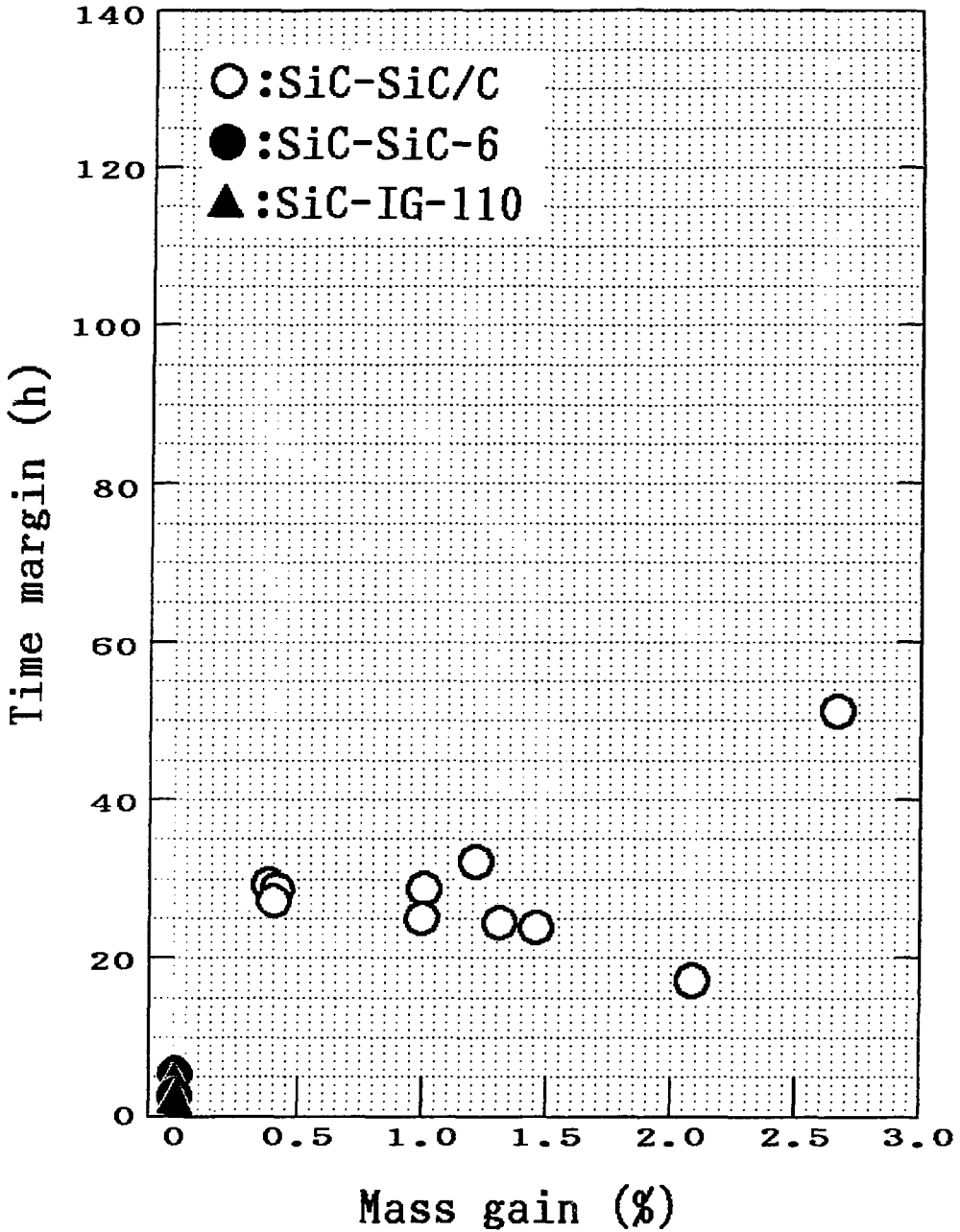


Fig. 8 Time margin from crack initiation to failure for surface SiC coating layer of the SiC-SiC/C as a function of mass gain of the SiC/C together with comparative data for both SiC coated graphite materials (without the SiC/C layer).

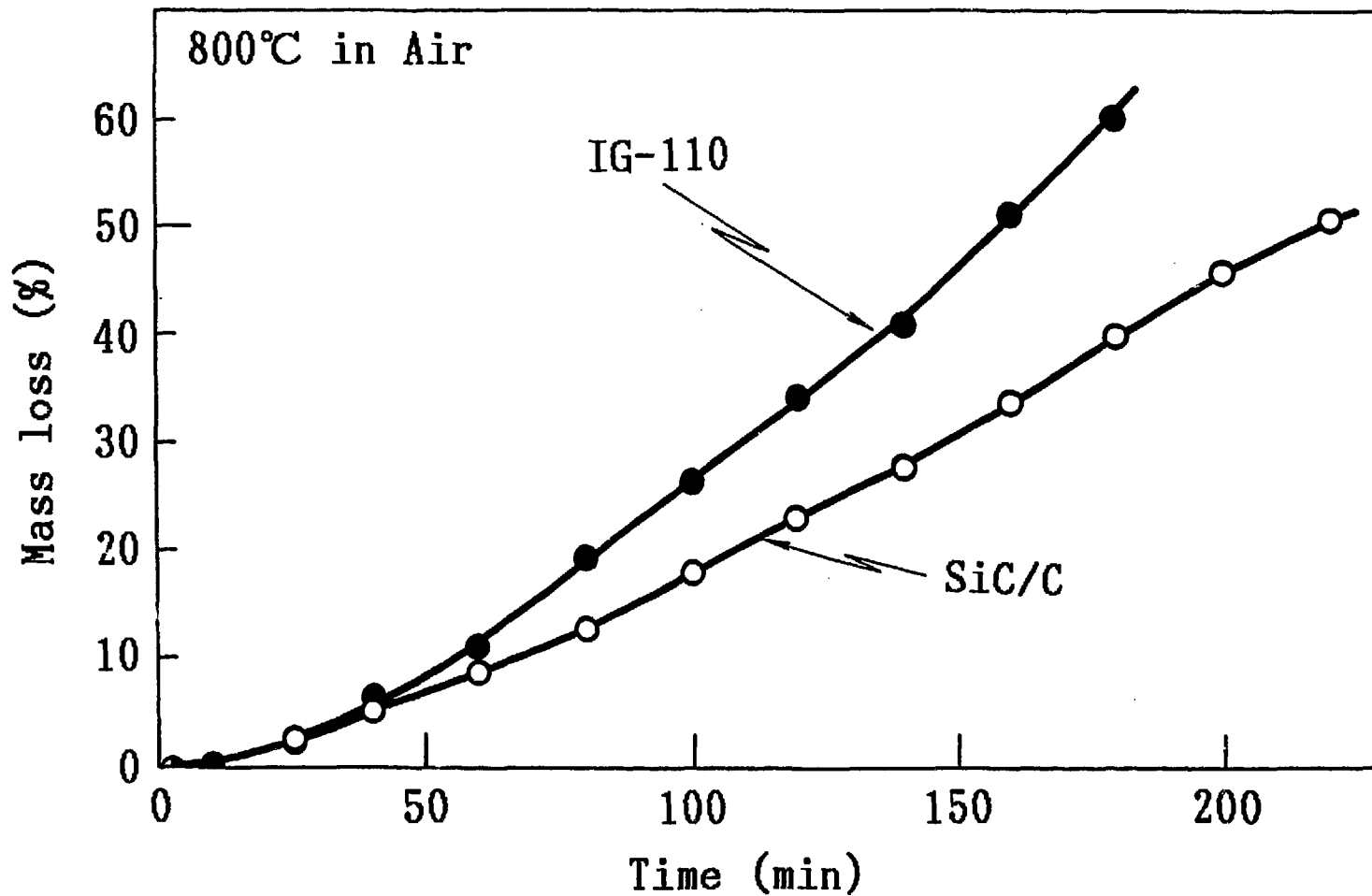
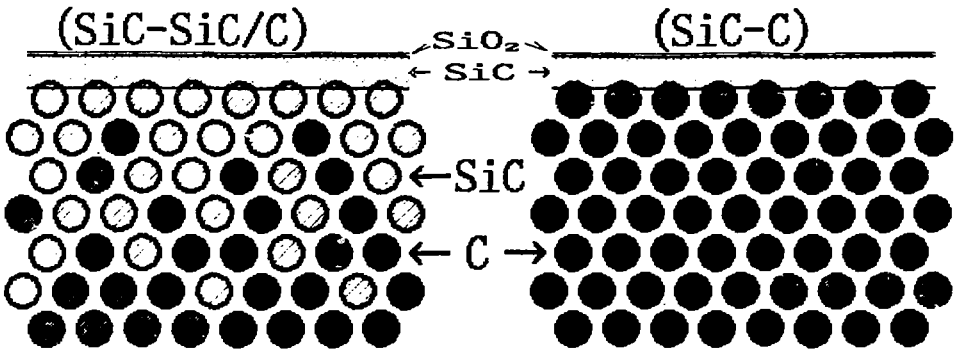
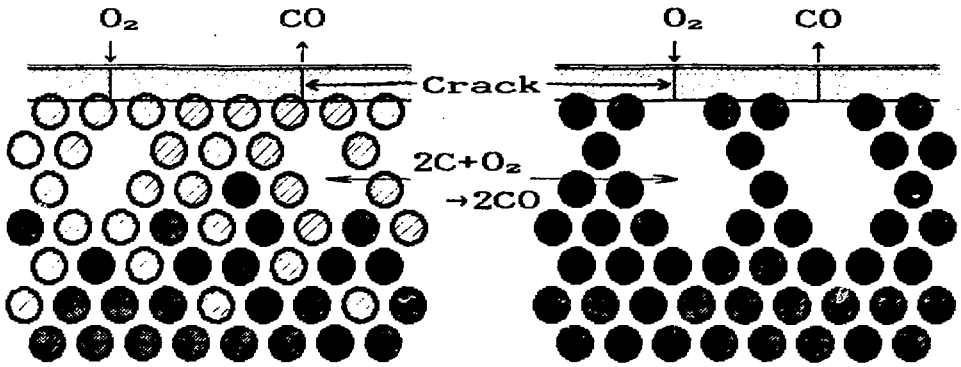


Fig. 9 Oxidation behavior of the SiC/C and IG-110 graphite, which is the substrate material of the SiC/C, at 800°C in air.

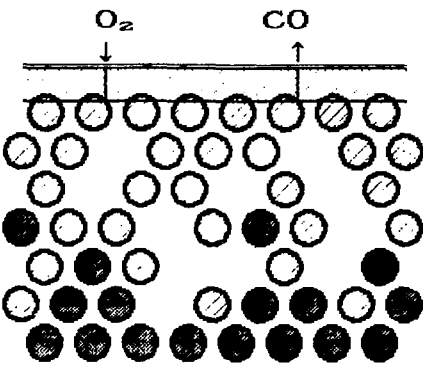
(1) No damage or failure



(2) Oxidation through cracks



(3) Continuation of (2)



(3) Failure

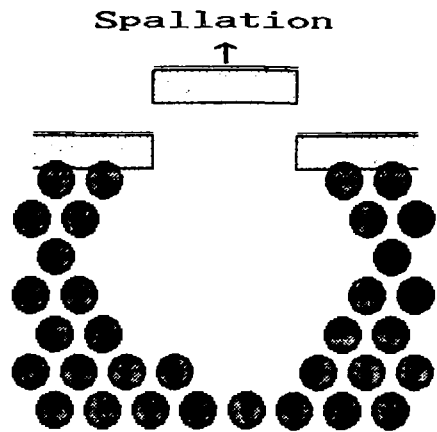


Fig. 10 Process from crack initiation to failure for surface SiC coating layers of the SiC-SiC/C and both SiC coated graphite (SiC-C).

国際単位系 (SI) と換算表

表1 SI基本単位および補助単位

量	名称	記号
長さ	メートル	m
質量	キログラム	kg
時間	秒	s
電流	アンペア	A
熱力学温度	ケルビン	K
物質	モル	mol
光度	カンデラ	cd
平面角	ラジアン	rad
立体角	ステラジアン	sr

表3 固有の名称をもつSI組立単位

量	名称	記号	他のSI単位による表現
周波数	ヘルツ	Hz	s ⁻¹
力	ニュートン	N	m·kg/s ²
圧力、応力	パスカル	Pa	N/m ²
エネルギー、仕事、熱量	ジュール	J	N·m
工率、放射束	ワット	W	J/s
電気量、電荷	クーロン	C	A·s
電位、電圧、起電力	ボルト	V	W/A
静電容量	ファラド	F	C/V
電気抵抗	オーム	Ω	V/A
コンダクタンス	ジーメンズ	S	A/V
磁束	ウェーバ	Wb	V·s
磁束密度	テスラ	T	Wb/m ²
インダクタンス	ヘンリー	H	Wb/A
セルシウス温度	セルシウス度	°C	
光束度	ルーメン	lm	cd·sr
照射度	ルクス	lx	lm/m ²
放射能	ベクレル	Bq	s ⁻¹
吸収線量	グレイ	Gy	J/kg
線量当量	シーベルト	Sv	J/kg

表2 SIと併用される単位

名称	記号
分、時、日	min, h, d
度、分、秒	° ' "
リットル	l, L
トン	t
電子ボルト	eV
原子質量単位	u

1 eV = 1.60218 × 10⁻¹⁹ J
1 u = 1.66054 × 10⁻²⁷ kg

表4 SIと共に暫定的に維持される単位

名称	記号
オングストローム	Å
バ	b
バ	bar
ガリ	Gal
キュリー	Ci
レントゲン	R
ラド	rad
レム	rem

1 Å = 0.1 nm = 10⁻¹⁰ m
1 b = 100 fm = 10⁻²⁸ m²
1 bar = 0.1 MPa = 10⁵ Pa
1 Gal = 1 cm/s² = 10⁻² m/s²
1 Ci = 3.7 × 10¹⁰ Bq
1 R = 2.58 × 10⁻⁴ C/kg
1 rad = 1 cGy = 10⁻² Gy
1 rem = 1 cSv = 10⁻² Sv

表5 SI接頭語

倍数	接頭語	記号
10 ¹⁸	エクサ	E
10 ¹⁵	ペタ	P
10 ¹²	テラ	T
10 ⁹	ギガ	G
10 ⁶	メガ	M
10 ³	キロ	k
10 ²	ヘクト	h
10 ¹	デカ	da
10 ⁻¹	デシ	d
10 ⁻²	センチ	c
10 ⁻³	ミリ	m
10 ⁻⁶	マイクロ	μ
10 ⁻⁹	ナノ	n
10 ⁻¹²	ピコ	p
10 ⁻¹⁵	フェムト	f
10 ⁻¹⁸	アト	a

(注)

- 表1 5は「国際単位系」第5版、国際度量衡局1985年所行による。ただし、1eVおよび1uの値はCODATAの1986年推奨値によった。
- 表4には海里、ノット、アール、ヘクタールも含まれているが日常の単位なのでここでは省略した。
- barは、JISでは流体の圧力を表わす場合に限り表2のカテゴリーに分類されている。
- EC閣僚理事会指令ではbar, barnおよび「血圧の単位」mmHgを表2のカテゴリーに入れている。

換算表

力	N (=10 ⁵ dyn)	kgf	lbf
	1	0.101972	0.224809
	9.80665	1	2.20462
	4.44822	0.453592	1

粘 度 1 Pa·s(N·s/m²) = 10 P(ポアズ)(g/(cm·s))
動粘度 1 m²/s = 10⁶ St(ストークス)(cm²/s)

圧	MPa (=10 bar)	kgf/cm ²	atm	mmHg(Torr)	lbf/in ² (psi)
	1	10.1972	9.86923	7.50062 × 10 ³	145.038
力	0.0980665	1	0.967841	735.559	14.2233
	0.101325	1.03323	1	760	14.6959
	1.33322 × 10 ⁻⁴	1.35951 × 10 ⁻³	1.31579 × 10 ⁻³	1	1.93368 × 10 ⁻²
	6.89476 × 10 ⁻³	7.03070 × 10 ⁻²	6.80460 × 10 ⁻²	51.7149	1

エネルギー	J (=10 ⁷ erg)	kgf·m	kW·h	cal(計量法)	Btu	ft·lbf	eV
	1	0.101972	2.77778 × 10 ⁻⁷	0.238889	9.47813 × 10 ⁻⁴	0.737562	6.24150 × 10 ¹⁸
	9.80665	1	2.72407 × 10 ⁻⁶	2.34270	9.29487 × 10 ⁻³	7.23301	6.12082 × 10 ¹⁹
	3.6 × 10 ⁶	3.67098 × 10 ⁵	1	8.59999 × 10 ⁵	3412.13	2.65522 × 10 ⁶	2.24694 × 10 ²⁵
	4.18605	0.426858	1.16279 × 10 ⁻⁶	1	3.96759 × 10 ⁻³	3.08747	2.61272 × 10 ¹⁹
	1055.06	107.586	2.93072 × 10 ⁻⁴	252.042	1	778.172	6.58515 × 10 ²¹
	1.35582	0.138255	3.76616 × 10 ⁻⁷	0.323890	1.28506 × 10 ⁻³	1	8.46233 × 10 ¹⁸
	1.60218 × 10 ⁻¹⁹	1.63377 × 10 ⁻²⁰	4.45050 × 10 ⁻²⁶	3.82743 × 10 ⁻²⁰	1.51857 × 10 ⁻²²	1.18171 × 10 ⁻¹⁹	1

1 cal = 4.18605 J (計量法)
= 4.184 J (熱化学)
= 4.1855 J (15 °C)
= 4.1868 J (国際蒸気表)
仕事率 1 PS (馬馬力)
= 75 kgf·m/s
= 735.499 W

放射能	Bq	Ci
	1	2.70270 × 10 ⁻¹¹
	3.7 × 10 ¹⁰	1

吸収線量	Gy	rad
	1	100
	0.01	1

照射線量	C/kg	R
	1	3876
	2.58 × 10 ⁻⁴	1

線量当量	Sv	rem
	1	100
	0.01	1